



## Neural dynamics necessary and sufficient for transition into pre-sleep induced by EEG NeuroFeedback



Sivan Kinreich<sup>a,c</sup>, Ilana Podlipsky<sup>c</sup>, Shahar Jamsky<sup>d</sup>, Nathan Intrator<sup>d</sup>, Talma Hendler<sup>a,b,c,\*</sup>

<sup>a</sup> Department of Psychology, Tel Aviv University, Tel Aviv 6997801, Israel

<sup>b</sup> Department of Physiology, Sackler Faculty of Medicine, Tel Aviv University, Tel Aviv 6997801, Israel

<sup>c</sup> Functional Brain Center, Wohl Institute for Advanced Imaging, Tel-Aviv Sourasky Medical Center, Tel Aviv 6423906, Israel

<sup>d</sup> School of Computer Science, Tel Aviv University, Tel Aviv 6997801, Israel

### ARTICLE INFO

#### Article history:

Accepted 12 April 2014

Available online 21 April 2014

#### Keywords:

Sleep onset  
External and internal awareness  
Salience network  
Thalamus  
EEG neurofeedback  
fMRI

### ABSTRACT

The transition from being fully awake to pre-sleep occurs daily just before falling asleep; thus its disturbance might be detrimental. Yet, the neuronal correlates of the transition remain unclear, mainly due to the difficulty in capturing its inherent dynamics. We used an EEG theta/alpha neurofeedback to rapidly induce the transition into pre-sleep and simultaneous fMRI to reveal state-dependent neural activity. The relaxed mental state was verified by the corresponding enhancement in the parasympathetic response. Neurofeedback sessions were categorized as successful or unsuccessful, based on the known EEG signature of theta power increases over alpha, temporally marked as a distinct “crossover” point. The fMRI activation was considered before and after this point. During successful transition into pre-sleep the period before the crossover was signified by alpha modulation that corresponded to decreased fMRI activity mainly in sensory gating related regions (e.g. medial thalamus). In parallel, although not sufficient for the transition, theta modulation corresponded with increased activity in limbic and autonomic control regions (e.g. hippocampus, cerebellum vermis, respectively). The post-crossover period was designated by alpha modulation further corresponding to reduced fMRI activity within the anterior salience network (e.g. anterior cingulate cortex, anterior insula), and in contrast theta modulation corresponded to the increased variance in the posterior salience network (e.g. posterior insula, posterior cingulate cortex). Our findings portray multi-level neural dynamics underlying the mental transition from awake to pre-sleep. To initiate the transition, decreased activity was required in external monitoring regions, and to sustain the transition, opposition between the anterior and posterior parts of the salience network was needed, reflecting shifting from extra- to intrapersonal based processing, respectively.

© 2014 Elsevier Inc. All rights reserved.

### Introduction

State of mind transitions, such as when one shifts their focus from the external world inward, are a common daily occurrence that manifests most strikingly as one falls asleep. Such transition may also occur spontaneously during mind wandering or when willfully regulating relaxation. Disturbance in sleep onset is prevalent among individuals suffering from depression or anxiety disorders (Hamilton, 1989; Neylan et al., 1998). However, healthy individuals are also prone to such difficulties, when experiencing daily concerns and tension (Augner, 2011) or as a result of aging (Foley et al., 1995).

The transition into pre-sleep is well defined by an EEG-based marker of a decline in the alpha amplitude followed by an increase in theta power while alpha remains low (De Gennaro et al., 2001; Hori et al.,

1994). The time at which theta becomes greater than alpha is referred to as the theta/alpha (T/A) “crossover” period and is assumed to indicate reduced vigilance and consciousness during the transition into a deep relaxation/pre-sleep state (Johnson et al., 2013; Peniston et al., 1993). This EEG marker of shifts in wakefulness has become a complementary measure for researchers using metabolic based imaging techniques such as fMRI and PET to indicate the transition into sleep. The modulation in EEG characteristics allows one to distinguish between arousal states revealing changes in the activity among large brain areas. Using this approach, fMRI and PET studies have found increased activity in the anterior cingulate cortex, the parietal cortices, and the temporal cortices (Olbrich et al., 2009), as well as in the bilateral hippocampus (Picchioni et al., 2008), while decreased activity was found in the frontoparietal cortices, the thalamus lobes (Kjaer et al., 2002; Olbrich et al., 2009), and the cerebellum (Kjaer et al., 2002). Although brain imaging studies generally indicate that many different brain regions are involved in the mental transition into pre-sleep, it is not yet clear which core neural network is necessary for such a transition while also taking into account on-going modulations of EEG markers.

\* Corresponding author at: Tel Aviv University, Tel Aviv 6997801, Israel. Fax: +972 3 6973080.

E-mail addresses: [hendlert@gmail.com](mailto:hendlert@gmail.com), [talma@tasmc.health.gov.il](mailto:talma@tasmc.health.gov.il) (T. Hendler).

The aim of the current study was to unveil the brain dynamics underlying this transition, using a well-established T/A EEG neurofeedback (EEG-NF) protocol (Peniston and Kulkosky, 1991). It has been repeatedly demonstrated that people can be trained to modulate their T/A ratio, yielding both physiological and psychological benefits (Hammond, 2011; Sokhadze et al., 2008). We therefore asserted that the T/A-EEG-NF training procedure can be used to investigate the trajectory of the mental transition into pre-sleep in a controlled fashion and within a short time period of a few minutes. For the validation of the reduced vigilance state we used heart rate variability (HRV) analysis. Vagal activity which acts to lower the heart rate was found to be a major contributor to the high-frequency (0.15 to 0.4 Hz) component of the power spectrum of heart rate variability (HR-HF) (Malik, 1996). Elevation of the HR-HF index (also referred to as parasympathetic HRV) has been linked to entering a state of relaxation (Malik, 1996, 2007) and early sleep stages (Calcagnini et al., 1994). Accordingly we assumed that there would be an increase in HR-HF power as individuals enter the pre sleep stage.

Simultaneous recording of fMRI provided high spatial resolution for the identification of the distinct brain network associated with the mental transition into pre-sleep. On the basis of previous imaging studies of arousal and attention, we hypothesized that brain areas related to external and internal monitoring and awareness would be essential during the initial stage of transition into sleep, possibly marked by the crossover time point. The thalamus in particular has been consistently found to be a key structure in relaying sensory signals and regulation of levels of attention and arousal states (Fiset et al., 1999; Ward, 2011). In addition, alpha rhythm has been repeatedly demonstrated as correlating with the thalamus activity as demonstrated in simultaneous combined imaging studies (Ben-Simon et al., 2008; Schreckenberger et al., 2004). Taken together we therefore expect that reduced EEG alpha power will be manifested in reduced thalamus fMRI activity. On the other hand, limbic/paralimbic medial and lateral temporal regions are suspected to be involved in the occipital theta modulation post crossover point. This is based on EEG studies showing that occipital theta is modulated specifically during the transition into pre-sleep (Peniston and Kulkosky, 1991) as well as sensitive to the processing of emotional stimuli (Aftanas et al., 2001; Uusberg et al., 2014).

Our findings show that T/A EEG-NF induces a state of pre-sleep that corresponds with an increased high-frequency heart rate variability (i.e. parasympathetic). In addition, successful training sessions portrayed distinct changes in fMRI activation related to pre- and post-crossover point, induced by either EEG alpha or theta modulations.

## Materials and methods

### Subjects

45 healthy subjects aged 24–37 years (22 males) signed an informed consent form approved by the ethical committees of the Tel Aviv Sourasky Medical Center and participated in a two-stage NF experiment; T/A EEG-NF training outside the MRI scanner and two sessions of T/A EEG-NF inside the MRI scanner.

### Experiment

#### EEG-NF practice outside the scanner

This experimental stage was designed to enable the subjects to become familiar with the neurofeedback procedure and setup. Participants were given a set of headphones (Trust International, Dordrecht, The Netherlands) to wear and an electrode cap was placed on their scalp. The NF electrodes (Oz, O1, O2) were chosen based on prior research using occipital electrodes (O1, O2) for theta/alpha NF relaxation sessions (Peniston and Kulkosky, 1991; Peniston et al., 1993). The Oz electrode was added to reduce signal artifacts. Participants were then asked to sit comfortably with their eyes closed in a quiet dark room

for the duration of the closed-loop feedback training (~15 min); T/A ratio modulation via EEG-NF. The closed-loop feedback procedure consisted of a continuous tune (a relaxing piano tune), that changed in volume every 3 s based on the real-time calculation of their T/A ratio (theta 4–7.5 Hz, alpha 8–12 Hz). The interval for calculating the feedback probe was chosen to fit the fMRI acquisition parameter of the TR (see below). Audio feedback values were determined in a pilot study (10 subjects), which resulted in 97% of the T/A values falling within the range of 0.2–2. This range was divided into 10 equal value ranges. The initial volume was adjusted individually according to the participants' request (about 60 dB SPL as measured by the headphone manufacturer equipment) and sound intensity feedback was calculated based on a criterion of 6 dB (the commonly accepted auditory dB distinction) inversely increasing or decreasing in proportion to the 10 possible values of the T/A power. T/A power values above 2 and below 0.2 were rounded to the closest feedback value. Subjects were instructed to close their eyes and try to relax as much as possible, while following the musical tune and using the shifts in volume as feedback for successful relaxation. Successful relaxation feedback was associated with a decrease in volume intensity. Real time EEG analysis for both practice and training stages was calculated using in-house software implemented in Matlab (Mathworks Inc, Natick, MA) and BrainProducts (Brain Products Inc, GmbH, Munich, Germany) software. Theta and alpha power were calculated every second, with the averaged value over time (3 s) and electrode signals (the three occipital electrodes) providing the basis for feedback.

#### EEG-NF training inside the scanner

A similar protocol to that used for training outside the scanner was applied twice, each time for 15 min, while participants were scanned in the MRI. The range of the T/A values was found to be similar inside and outside of the scanner and led to similar feedback calculation. Sound production and delivery were provided via MRI compatible headphones with active noise cancellation (Optoacoustics Ltd, Moshav Mazor, Israel). To improve NF efficacy, three individualized electrodes with the highest T/A amplitude during training were selected out of a total of eight occipital electrodes (OZ, O1, O2, P3, PZ, P4, CP1, CP2) (for set-up illustration see Kinreich et al., 2012).

#### Data acquisition

##### EEG

Electrical brain signals were recorded using an MR compatible EEG system with a 32 electrode cap (including one electrocardiogram electrode) (BrainAmp MR and BrainCap MR, Brain Products Inc). Electrode locations followed the international 10–20 system, a reference electrode was located between Fz and Cz, and the sampling rate was 5 kHz.

##### fMRI

MRI scans were performed on a 3.0 Tesla MRI scanner (GE Signa EXCITE, Milwaukee, WI, USA) with an eight channel head coil. fMRI was performed with the gradient echo-planar imaging (EPI) sequence of functional T2\*-weighted images (TR/TE/flip angle: 3000/35/90; FOV: 20 × 20 cm; matrix size: 128 × 128) divided into 39 axial slices (thickness: 3 mm; gap: 0 mm) covering the whole cerebrum. Anatomical 3D spoiled gradient echo (SPGR) sequences were obtained with high-resolution 1-mm slice thickness (FOV: 250 mm; matrix: 256 × 256; TR/TE: 6.7/1.9 ms).

#### Data analyses

##### EEG

##### Preprocessing

Matlab (Mathworks Inc, Natick, MA) and EEGLAB ((Delorme and Makeig, 2004)) were used for all calculations. Removal of MR gradients

and cardio ballistic artifacts included a FASTER algorithm (Niazy et al., 2005) implemented in the FMRIB plug-in for EEGLAB. To reduce computational complexity the EEG signal was subsequently down-sampled to 250 Hz. Time frequency representation of the EEG was calculated using the Stockwell transform (Stockwell et al., 1996) with a time resolution of 1/250 s and a frequency resolution of 0.3 Hz. The alpha and theta instantaneous power was then extracted from the time–frequency transform as the average power across the relevant bands. Finally, the theta/alpha instantaneous power ratio was derived as a sample-wise division of the relevant powers.

#### Successful/unsuccessful session categorization

To determine success in NF training we computed the envelope (implemented by Matlab using the Hilbert Transform) of the T/A power ratio and calculated the proportion of time in which the envelope was above 1. A session was defined as successful when the envelope was above 1 between 20% and 80% of the time, including at least 80 consecutive TRs. This indicated which subject sessions began with wakefulness and entered a state of pre-sleep for at least 4 min (Johnson et al., 2013). A session was defined as unsuccessful when the T/A power envelope was below 1 for at least 80% of the time with at least 80 consecutive TRs (see individual examples in Fig. 1). 40 sessions that did not match these criteria were excluded from the study. Fifteen additional sessions were excluded due to various technical problems during scanning (see fMRI preprocessing & analysis) and another five sessions were excluded due to group criteria requiring that each participant may be part of only one group (i.e. successful or unsuccessful). In total the two experimental groups included 15 successful and 15 unsuccessful sessions.

#### The crossover time point

The crossover point was defined as the time in which the envelope function of the T/A power signal changed from below one to above one. This value was calculated using a 60 second running window on the envelope function of the T/A power. The size of the running window was chosen to reduce phasic activity artifacts. The signal within each window was then averaged and the window with a value closest to 1 was recorded as the transitional “crossover time period” with its midpoint

as the transitional “crossover time point”. Naturally, both theta and alpha underwent a signal power change around the T/A crossover time. In order to calculate the theta and alpha transitional time point we applied smoothing algorithms (5-point moving average) followed by a calculation of the global minimum. The individual data points were visually inspected and corrected for outlying artifacts. The EEG power modulation per band during pre- and post-crossover points was used for further fMRI regression analysis. For the purpose of the theta and alpha modulation analysis a full spectrum of the frequencies (FFT) was calculated for the pre- and post T/A crossover time point.

#### Heart rate

For the purpose of HR variability (HRV) analysis, electrocardiogram (ECG) signal preprocessing included removal of MR gradient artifacts and detection of ECG R peaks using a FMRIB plug-in for EEGLAB (Raz et al., 2012). Further irregular beats due to motion artifacts were corrected via visual inspection (see (Raz et al., 2012)). The inter-beat intervals were obtained as differences between successive R-wave occurrence times. A linear interpolation was used to obtain an equidistantly-sampled time series of RR intervals. Due to motion artifacts, only 10 successful and 10 unsuccessful sessions were included in the final HR analysis, for which a reliable R peak signal could be detected in all sessions. Fourier transform was applied to the RR interval time series to obtain the HRV power spectrum. The parasympathetic HRV index was calculated as the power of the high frequency band of the HRV spectrum (0.15–0.4 Hz) (Fig. 2A for one subject example).

To validate the relaxation state we correlated the modulation over time of the T/A power ratio and the modulation of the parasympathetic peak power. For 10 subject sessions in the successful group and 10 subject sessions in the unsuccessful group, both signal time courses (the power modulation over the time of the scan of T/A and the high frequency band of the HRV spectrum) were divided into seven equal time intervals and averaged over each interval creating a seven-point vector. For each individual we correlated the seven point HRV & T/A vectors. Using Fisher’s transform, the individual correlation was converted to

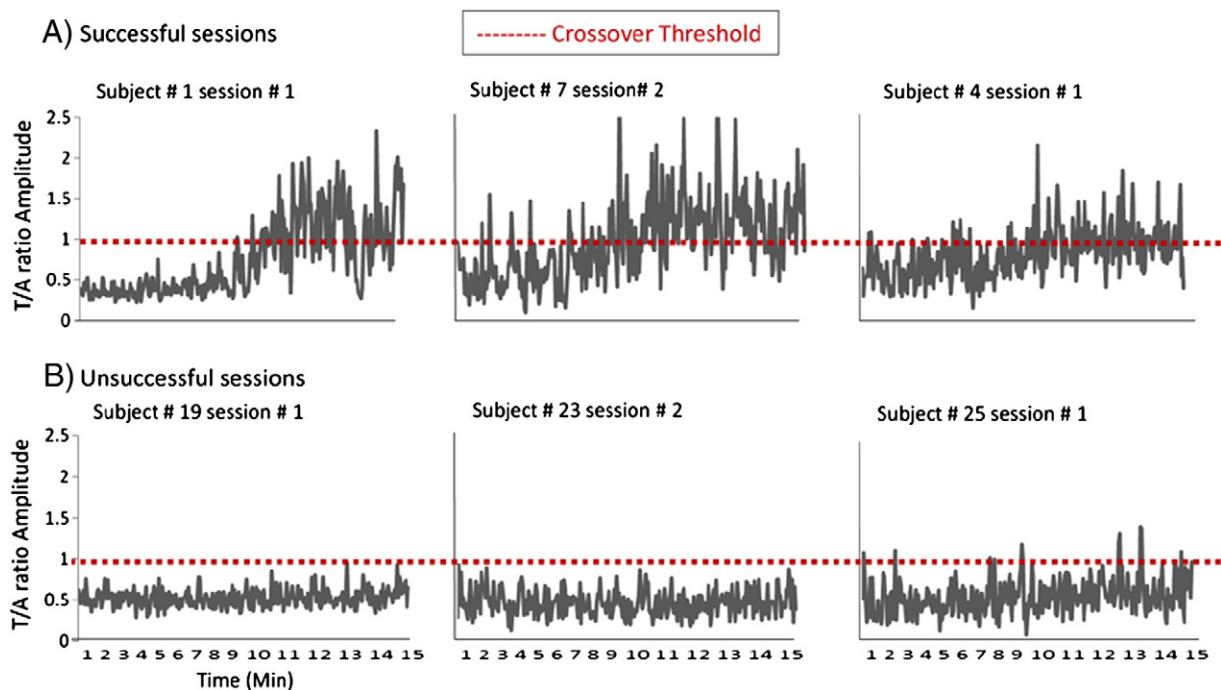


**Fig. 1.** Grouped sessions by T/A EEG-NF modulation time courses. Each session was categorized as successful or unsuccessful according to the predefined criterion of an increase in the T/A ratio above 1 (red dotted line). Three signal time courses are depicted for sessions in the successful group (A), and the unsuccessful group (B). The signal time courses of the successful sessions illustrate the variability found in T/A power modulation throughout the training with a crossover point indicated by an increase in the T/A ratio above 1.

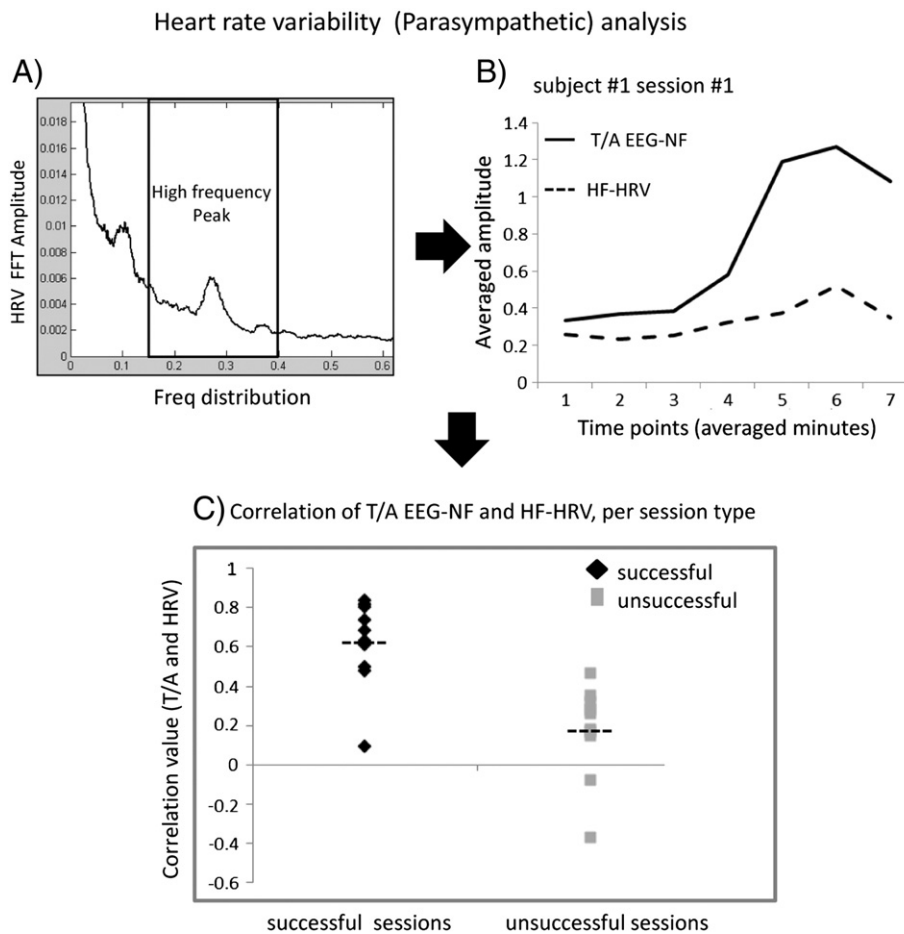


**Fig. 2.** Heart rate variability (parasympathetic) analysis. A. The Fourier transform of the heart rate measurement for subject #1 shows the common high- and low-frequency peaks of the power spectrum. B. Correlations of the 7 averaged values of the T/A EEG-NF progression throughout training for subject #1 and the corresponding averaged HR-HF spectrum changes ( $R = 0.8810$ ,  $P = 0.0088$ ). This successful session shows high correspondence between HR parasympathetic power and T/A power modulation. C. Comparison of the correlation between T/A EEG-NF and HR-HF values for successful (diamonds) and unsuccessful (squares) sessions ( $n = 20$ ). A direct comparison shows higher correlation values for successful sessions. Mean value of the correlation for each group (black dotted lines) (two-tailed  $t$ -test,  $p < 0.00005$ ).

z-scores. The z-scores from each participant were then entered into the group-level analysis for  $t$ -test assessment.

## fMRI

### Preprocessing

Preprocessing included slice timing correction, motion correction (head motion exclusion criteria included gross translational motion that exceeded 3 mm on any axis—15 sessions were excluded), normalization into Talairach space, and spatial smoothing using a 8-mm FWHM Gaussian kernel (Brainvoyager, Brain Innovation, Maastricht, The Netherlands).

### Successful/unsuccessful GLM regressors

Regression maps were obtained for each successful session based on four regressors including 80 time points each (i.e. 4 min). Two regressors were defined as the alpha power modulation and two as the theta power modulation immediately before and after the crossover time point. For both bands, the pre-crossover period was determined as 4 min up to the crossover time point and the post-crossover period was determined as 4 min from the crossover time point onward (for one subject example see Fig. 3). The length of 80 time points was chosen to limit the regressor to the time of the change (see example in Fig. 3). The four individualized regressors were first z-scored and then convolved with the hemodynamic response function (shift in

time  $\Delta t = 6$  s) for the GLM fMRI analysis; theta decreased, theta increased, alpha decreased, and alpha flattened.

For each unsuccessful session we defined a regressor of the same length (80 TRs each) based on either alpha or theta power modulation. Since the unsuccessful signal did not show the unique modulation of theta and alpha crossover time point accompanied by achieving a pre-sleep state, we defined the regressor as the time window in which the signal showed the least amount of modulation. For that we calculated the signal change using a sliding window of 80 time points, in which we searched for the time period with the smallest standard deviation. Thus two regressors were created, one for the alpha signal and one for the theta signal, convolved with the HRF function. Note that regressor onset time, as well as its temporal shape, was different for each participant and session. GLM whole brain regression analysis included four random effect group comparisons between successful and unsuccessful sessions.

Region of interest analysis was performed for the four regression contrast maps (pre-post crossover periods, for alpha and theta). The subjects' averaged spatial  $t$ -value maps obtained for each period and band were calculated by identifying the peak activation voxel for each of the three most significant regional activations in each specific map. The averaged signal of each ROI was calculated using the peak of activation as a seed coordinates for a Gaussian smoothing filter with a radius of 6 mm (thus creating the same volumes for all the ROIs). The signals were then averaged across ROIs (Table 1 shows the region locations per map). Next, we calculated the averaged percent signal change and

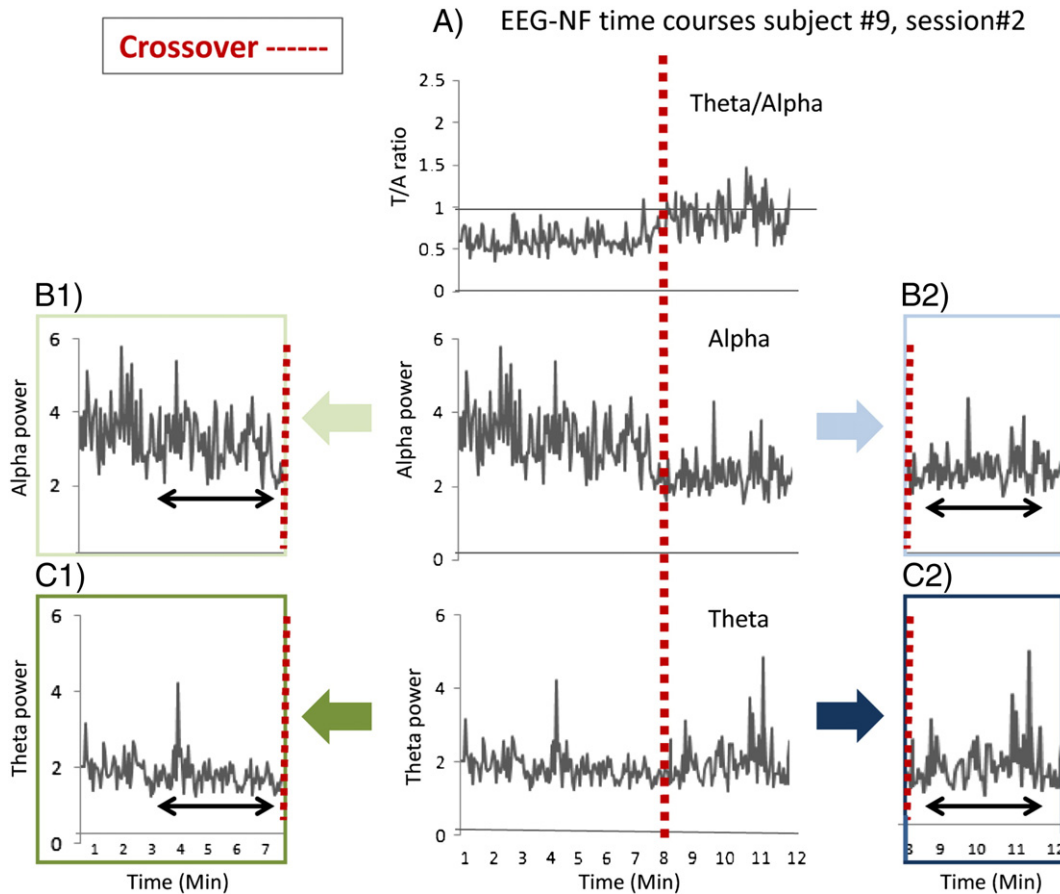


**Fig. 3.** Pre- and post-crossover EEG modulation. Upper trace: The T/A ratio signal time course for one subject's session, with the "crossover" at ratio = 1 (perpendicular red dotted line). Lower traces show the alpha and theta power modulation that correspond to this ratio calculation. It is clear that their power modulation shows different patterns over the two sides of the crossover (pre- and post-crossover). While alpha shows pre-crossover decrease and then stays flattened, theta shows pre-crossover decrease and post-crossover increase. We used these robust EEG characteristics to formulate four different fMRI regressors as presented in the boxes: *Pre-crossover* alpha and theta modulation (B1 & C1; light and dark green rectangles, respectively), and *Post-crossover* alpha and theta modulation (B2 & C2; light and dark blue rectangles, respectively). Regressor length is 4 min bordered by the crossover time point (black arrow below the signal).

its variability for each crossover period and band: maximal percentage increase, maximal percentage decrease, and maximal variance. These measures were calculated using a 30 s running window on the averaged signal relative to a 30 s period at the beginning of each NF session. The size of the running window was chosen to reduce phasic activity artifacts. A *t*-test was then performed to compare successful from unsuccessful sessions on the averaged signal change and on the variance.

## Results

Simultaneous fMRI and EEG-neurofeedback were used to initiate and explore the mental state transition from wakefulness to pre-sleep. The purpose of this study was to unfold the core networks involved in the transition and, specifically, to pinpoint the essential neural dynamics for the change. Thus, we chose to contrast successful vs. unsuccessful transitions into pre-sleep sessions identified by the theta/alpha (T/A) ratio crossover time point.

### General overview of the results

1) Successful and unsuccessful NF sessions were identified based on the temporal EEG marker of theta increased over alpha and validated by the increase in the parasympathetic response. 2) Whole brain fMRI analysis revealed four distinguishable patterns of correlation with the pre- or post crossover EEG changes, representing the neural dynamics during the transition into pre-sleep. 3) Activation analysis of the unfolded four patterns included a comparison between successful and

unsuccessful NF sessions suggesting brain region dynamics during the transition into pre-sleep.

### Categorization of NF sessions by EEG and HR

EEG analysis revealed two T/A ratio modulation patterns for each session type: gradual increase or no increase, indicating successful or unsuccessful transition into pre-sleep ( $n = 15$  each). Fig. 1A and B demonstrates the modulation of the individual EEG T/A ratio for 3 successful and 3 unsuccessful sessions. HRV measures served as validation for relaxation/pre-sleep training success. Fig. 2B shows a significant correlation [ $R = 0.8810$ ,  $P = 0.0088$ ] between the HR parasympathetic index and the calculated T/A ratio for one successful session. Moreover, Fig. 2C shows that the correlation scores for the T/A ratios and HRV were higher for successful than unsuccessful sessions (two-tailed *t*-test,  $p < 0.00005$ ).

### fMRI regression maps per EEG-T/A crossover period and band

Within the framework of successful training, crossover time points were calculated from the time courses of the alpha and theta power and T/A ratio for each NF session. As expected theta and alpha crossover time points were found to largely overlap with the T/A ratio 60 second time window across sessions and individuals (supplementary Fig. S1), creating two different time periods (i.e. pre- and post crossover) for each of the relevant EEG bands; alpha and theta (see Methods and Fig. 3). Full spectrum analysis demonstrates different modulations of

**Table 1**  
Selected peak of activation for each of the four networks.  
ROI peak of activation per EEG crossover period and band.

	Side	x	y	z	Voxel no.	t-value
<i>Pre-crossover alpha</i>						
Medial thalamus	L	-7	-19	14	932	6.19
	R	5	-18	12	352	5.71
Putamen	R	27	-3	11	417	5.7
Caudate	R	13	14	15	605	5.66
<i>Pre-crossover theta</i>						
Cerebellum vermis	L	-4	-58	-30	969	6.73
Ventral tegmental area	L	-1	-16	-8	273	5.89
Superior colliculus	R	5	-32	-6	210	5.7
Cerebellum anterior vermis	L	-1	-48	-15	668	5.65
Parahippocampal	R	23	-38	-9	706	5.18
Hippocampus	L	-32	-17	-13	389	4.872
BA 19	L	-16	-57	-5	300	4.7
ACC BA24	L	-3	31	2	427	4.6
<i>Post-crossover alpha</i>						
Medial thalamus	L	-7	-21	13	688	8.09
	R	7	-17	12	748	7.7
PCC BA23	L	-3	-31	26	409	6.13
Putamen	R	23	-3	14	128	6.3
Caudate	R	15	11	16	591	6.042
Dorsal ACC BA32	R	3	15	41	334	5.7
Rostral ACC	R	3	37	23	489	5.69
Anterior insula	R	33	15	12	346	5.5
	L	-27	18	3	258	4.55
<i>Post-crossover theta</i>						
Posterior insula	L	-33	-21	11	366	6.39
	R	29	-19	15	107	5.014
PCC BA31	R	14	-26	38	117	4.57

$p < 0.05$  FDR corrected.

theta and alpha across the crossover time point (i.e. high alpha amplitude before the crossover time point changes to increase in theta after, supplementary Fig S2).

To probe the fMRI activity that underlies EEG modulation per band, the pre-post crossover periods from successful sessions were contrasted with unsuccessful periods (see *Methods*). GLM analysis with pre-crossover alpha power modulations as a regressor revealed fMRI activation in the bilateral medial thalamus, putamen, and caudate nuclei (Fig. 4B1); theta power modulations as a regressor revealed fMRI activity in the cerebellum vermis, superior colliculus, ventral tegmental area (VTA), hippocampus, and parahippocampal area (Fig. 4C1). The post-crossover alpha power modulations correlated with fMRI activity in the medial thalamus as well as within the posterior cingulate cortex (PCC) (BA 23) and in dorsal and rostral ACC (Fig. 4B2). Note that changes in pre and post crossover alpha related fMRI activation largely overlap within the medial thalamus and striatum areas (i.e. right caudate and right putamen) (supplementary Fig. S3). Lastly, the theta power modulations correlated with fMRI activity in the posterior insula and mid PCC (BA31, Fig. 4C2). ROI coordinates of the four networks are shown in Table 1.

#### fMRI regional analysis per crossover period and band

To further characterize the fMRI activity modulation that underlies each correlation map, regional signal activity changes and their variance were evaluated (see *Methods*). Fig. 5 presents the average percent signal change and variance for each period and band related network, separately for successful and unsuccessful sessions. During the pre-crossover period, the alpha network exhibited a decrease in fMRI activity for successful sessions only, while the theta network showed an increase in activation for both successful and unsuccessful sessions (Fig. 5B1 and C1). During the post-crossover period a decrease in activity in the alpha network and an increase in variance in the theta network were found for successful sessions only (Fig. 5B2 and C2). These

findings are summarized in Fig. 6. Interestingly, alpha and theta post crossover networks include two cingulate cortex ROIs in close proximity; i.e. the posterior cingulate cortex (-3, -31, 26) and the more mid cingulate cortex (14, -26, 38), respectively. Their opposing activation (see Fig. 5) suggests different roles during transition into pre-sleep.

## Discussion

Using fMRI simultaneously with EEG-NF provided a unique opportunity to explore and unfold the various neural dynamics that underlie successful transition from wakefulness to pre-sleep. T/A crossover was used to categorize sessions as successful or unsuccessful while an increased HR parasympathetic index verified the relaxed state of the successful ones. The fMRI activity suggests that the mental transition into pre-sleep requires two-staged interleaved processes. The initiation of transition was driven by reduced activity within the brain systems involved in externally driven sensations and monitoring (e.g. thalamus), while the continued transition into pre-sleep called for increased activity among areas involved in interception and internal homeostasis (e.g. the posterior insula).

#### Pre-crossover EEG related fMRI activity modulation

Alpha modulation during the pre-crossover period corresponded with a decrease in activity among regions involved in sensory gating such as the medial thalamus, caudate and putamen nuclei. These regions have previously been associated with changes in neural activation when transitioning into sleep or while resting with eyes closed (Larson-Prior et al., 2011; Olbrich et al., 2009). Importantly, deactivation in these areas clearly differentiated between successful and unsuccessful EEG-NF sessions (Fig. 5B1), thus indicating conditions that are likely necessary to induce a transition into pre-sleep as well as to fall asleep.

Specifically, the observed deactivation of the medial thalamus may reflect its hypothesized role as a key component in the regulation of levels of awareness towards external stimuli (Ward, 2011). In a recent single unit recording study on monkeys, the central thalamus was found to regulate task performance through brief changes in firing rates and spectral power, correlated with increases in attentional effort (Schiff et al., 2013). Human studies found that as individuals under anesthesia entered an unconscious state a decrease in cerebral blood flow within the bilateral medial thalamus occurred (Fiset et al., 1999). Schiff et al. (2013) recently suggested that medial thalamic activation may reflect a limbic gating mechanism involved in modifying interactions between input and output of different brain substrates, leading to the regulation of arousal and allocation of attentional resources. Regarding the transition into pre-sleep, decreased activity in this network may reduce the externally-driven allocation of attention and awareness thus enabling an internal shift of directing attention.

The theta modulation during successful pre-crossover NF sessions corresponded with an increase in fMRI activity among major regulatory nodes in distributed subcortical regions within the midbrain (e.g. ventral tegmental area, VTA), cerebellum and the hippocampal areas (see Fig. 5 and Table 1). Although this modulation in activity was found to be more pronounced during successful sessions, regional activation analysis indicated increased activation during unsuccessful sessions as well, suggesting that the change in activity within these systems was necessary, but not sufficient, for successful transition into pre-sleep.

Specifically, the VTA; a central dopaminergic relay nucleus in the midbrain, receives visual input from the superior colliculus which has been associated with controlling automatic saccadic eye movements and eye-head movement coordination (Coizet et al., 2003; Wang et al., 2002). The anterior cerebellum vermis, on the other hand, has been shown to be involved in modulating autonomic responses related to cardiovascular and respiratory functions (Ghelarducci and Sebastiani, 1996) and in monkeys it was also found to be involved in the regulation of whole-body posture and locomotion (Coffman et al., 2011). Thus, the

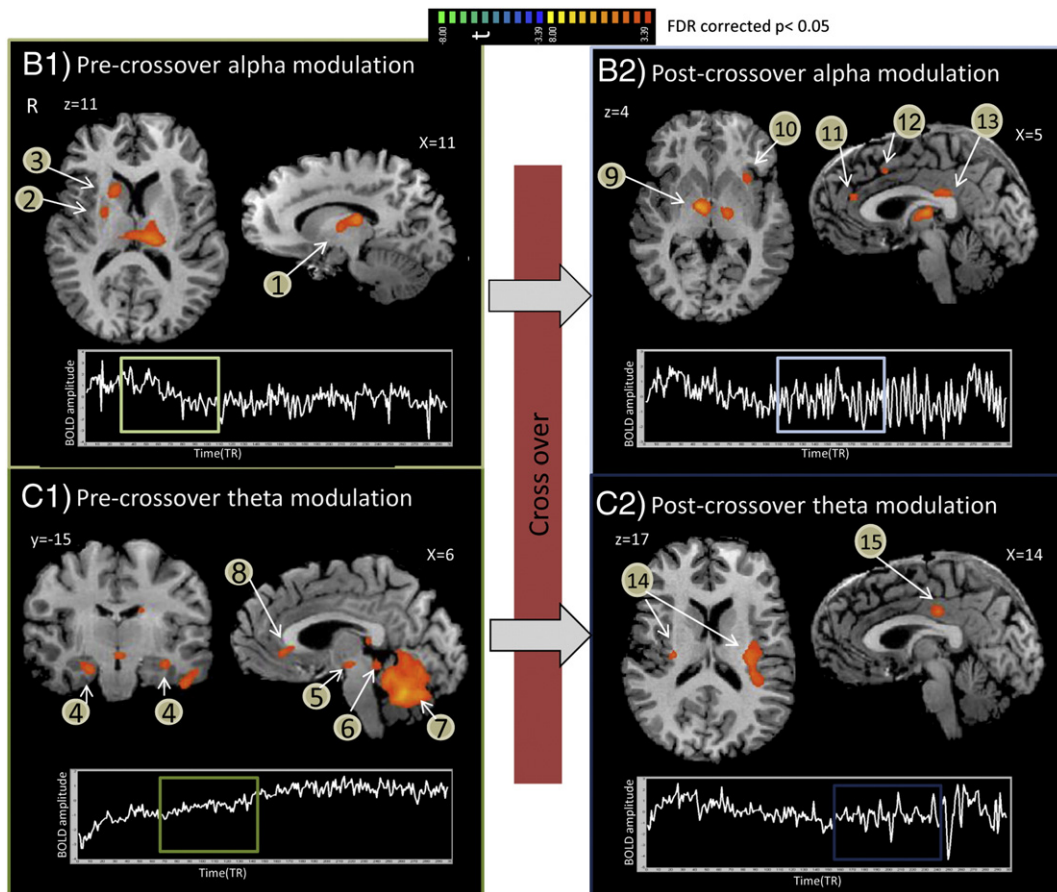


**Fig. 4.** GLM whole brain group analysis. Comparing successful ( $n = 15$ ) vs. unsuccessful ( $n = 15$ ) sessions revealed the network associated with the progression into pre-sleep as related to pre- and post-crossover theta and alpha modulation, respectively. B1. BOLD activation obtained by the pre-crossover alpha modulation: 1. bilateral medial thalamus, 2. right putamen, 3. right caudate. C1. BOLD activation obtained by the pre-crossover theta modulation: 4. bilateral hippocampus, 5. ventral tegmental area (VTA), 6. right superior colliculus, 7. vermis cerebellum, 8. ventral ACC. B2. BOLD activation obtained by the post-crossover alpha modulation: 9. bilateral medial thalamus, 10. anterior insula, 11. rostral ACC, 12. dorsal ACC, 13. posterior CC. C2. BOLD activation obtained by the post-crossover theta modulation: 14. bilateral posterior insula, 15. BA 31. The three most significant ROIs for each network were used to create the time course of the averaged BOLD signal (e.g. one subject–BOLD signal acquired from the peak of activation voxel after z-transform denoted under each network map). Green and blue rectangles for the pre- and post crossover periods respectively, mark the regressor time frame for the corresponding network.

functions of these deep brain areas are closely related to the well-documented physiological and behavioral effects that accompany reduced arousal such as: reduction in muscle tonus (Kleitman, 1963), decrease in heart rate and changes in respiration (Trinder et al., 2001; Worsnop et al., 1998), as well as the appearance of slow eye movements (Hiroshige and Miyata, 1990; Marzano et al., 2007). Lastly, the involvement of the hippocampus and parahippocampus in this initial stage of mental transition is particularly intriguing, as these brain regions have not traditionally been linked to arousal modulation and relaxation. However, recent intracranial studies on epileptic patients have shown a continuous increase in activity within the parahippocampal area during the wake–sleep transition suggesting that the parahippocampus mediates the onset of hypnagogic hallucinations, just prior to falling asleep (Bodizs et al., 2005), with the hippocampus enabling sleep-related memory consolidation (Moroni et al., 2008).

#### Post-crossover EEG related fMRI activity modulation

Alpha modulation during the post-crossover period corresponded with a continued deactivation of the medial thalamus–striatum network indicating the importance of maintaining externally-tuned awareness at a low level in order to remain in the transition of falling asleep. Deactivation was also found within the PCC, a key hub of the default mode network. Recent hypotheses regarding the default mode network suggest that it plays a role in monitoring external stimuli during task-free periods (Gilbert et al., 2007; Shulman et al., 1997), thus supporting

a broad low-level focus of attention to unexpected external events during rest times (Buckner et al., 2008). Of particular interest is the additional deactivation found in the ACC and anterior insula, major nodes of the salience network (Menon and Uddin, 2010). This finding supports previous evidence that the ACC–AI connection is uniquely responsible for externally-oriented attention for the detection of prominent stimuli in order to guide other networks accordingly (Menon and Uddin, 2010). In the context of mental transition from rest to pre-sleep, the deactivation of these networks indicates the importance of reducing activity among on-going external awareness/monitoring systems in order to make the shift inward.

The theta-related fMRI network modulation among individuals who successfully entered the pre-sleep stage showed an increase in variance. Specifically, there was an increased variance in the bilateral posterior insula (PI) and mid PCC (see Table 1 and Fig. 5). In fact, an increase in variance was also evident during the post-crossover period for the alpha-related fMRI activation. The finding of increased variance while entering sleep is consistent with previous fMRI studies showing it in largely distributed networks (Horowitz et al., 2008; Larson-Prior et al., 2009).

The inclusion of PI and mid PCC in the theta related fMRI modulation fits a recently suggested model of the “posterior salience network” unfolded in a functional connectivity analysis during rest (Shirer et al., 2012). PI, specifically, was implicated as an important interoceptive node, regulating central somatic awareness, physiological reactivity and internal homeostatic states (Menon and Uddin, 2010; Xue et al.,

Regional fMRI activation per EEG band modulation period

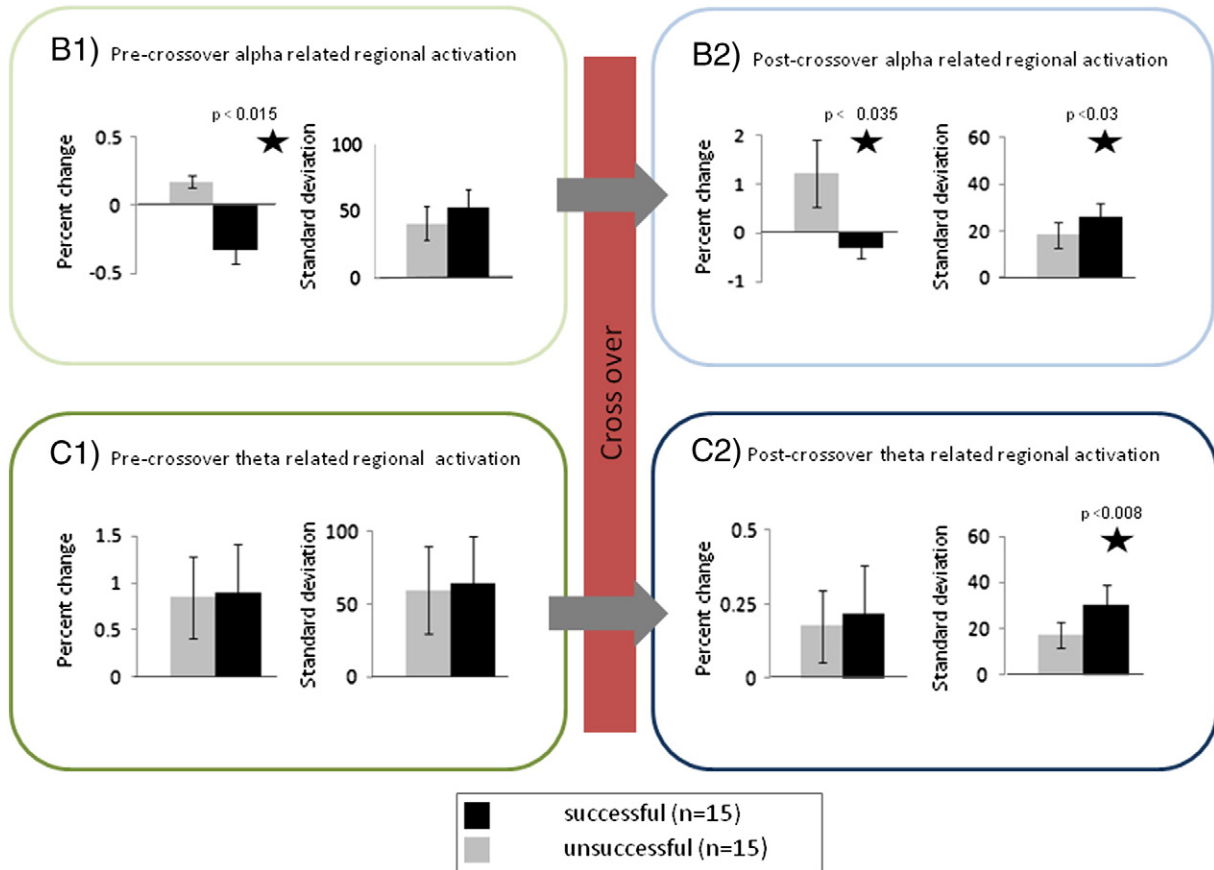


**Fig. 5.** Percent signal change and standard deviation group analysis. Data obtained from individual BOLD signals (average over the three most active regions in each networks, see Fig. 4). The averaged values per time period relative to crossover and responsiveness were compared via *t*-test analysis. Bars indicate B1 & C1: comparisons of pre-crossover alpha and theta modulation networks, respectively. B2 & C2: comparisons of post-crossover alpha and theta modulation networks, respectively. Stars mark significant comparisons between successful and unsuccessful sessions per period. The results demonstrate the critical factors for entering the crossover phase for pre-sleep; reduction in alpha-related pre-crossover network activity.

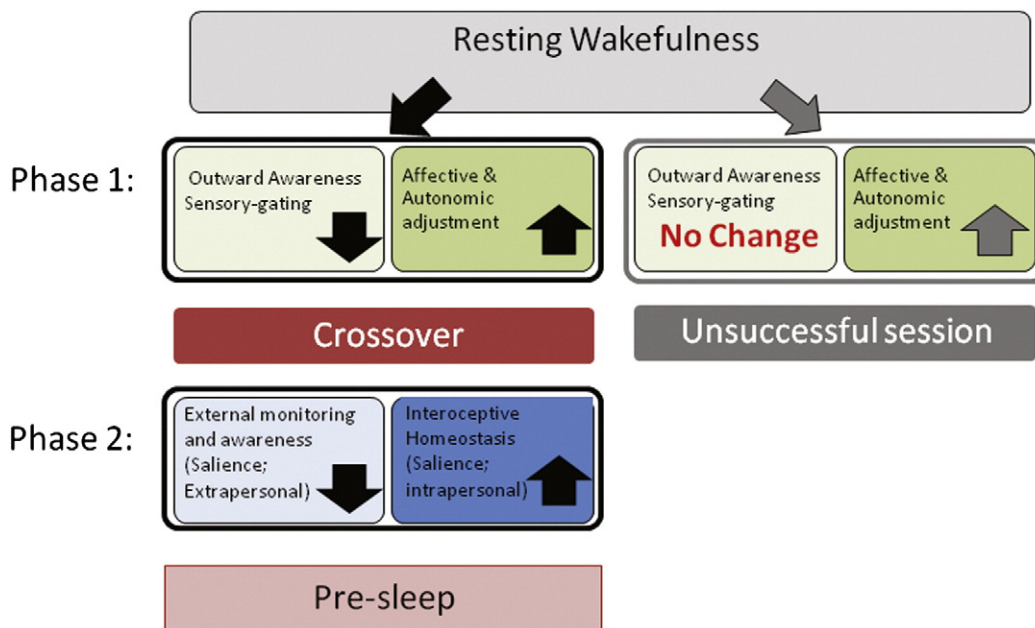


**Fig. 6.** Brain model of the transition into pre-sleep. The model describes the brain dynamics involved in the progression into a pre-sleep state. It suggests the necessary and sufficient conditions for transitioning into such a state. During the first phase upon closing one's eyes a sufficient condition is an increase in activity of autonomic-control and affective/cognitive homeostasis networks (successful & unsuccessful phase 1, right dark green squares). Simultaneously reduced activity in the system associated with external awareness was revealed. This modulation is an essential condition, as unsuccessful sessions did not show decreased activity in this network (successful & unsuccessful left light green square first phase). Only successful phase 1 sessions show relaxation-related brain activities at phase 2 of the model, which requires a maintained reduction in the activity of external awareness and an increase in the variance of both external awareness and the interoceptive homeostasis network (successful, phase 2 left light/dark blue squares).

2010) suggesting that the hypothesized temporal lobe related theta modulation refers to an internally generated emotional state (e.g. relaxation). In accordance with the PI role in interoception, the mid PCC was found to be involved in processes related to self integrity such as anticipation of pain (Lyons and Zelazo, 2011) and self judgment reflecting inward self-referral dynamics (Han et al., 2010). In the context of pre-sleep this connection might play a role in inward homeostasis and self related processing.

### An integrative account

This research provides experimental evidence of the relationship between brain activity, mental state and EEG modulation. Fig. 6 outlines a possible neural model for the transition into pre-sleep. Alpha and theta distinctive modulation during transitional processes revealed opposite involvement of the two parts of the salience network; the AI and ACC underwent deactivation together with the sensory gating system, while the PI and PCC were activated simultaneously.

We present here a novel attempt to delineate functional parts of the salience network, which are possibly related to intrapersonal/extrapersonal aspects of awareness. As previously suggested, the salience network may play a role in switching between brain states; e.g. default versus executive (Sridharan et al., 2008). In the present study, the deactivation of the AI and ACC along with deactivation in the sensory gating system may reflect a refocusing from external to internal attention (Menon and Uddin, 2010), while the activation of the PI and PCC following enhanced activation in the VTA, cerebellum, and hippocampus reflects increased engagement in interoceptive, intrapersonal processes (Menon and Uddin, 2010). The importance of this suggested neural model is that it directs diagnostics or intervention to specific brain areas. For example, the alleviation of social anxiety could involve modulating the externally-oriented salience network, while alleviation of depressive ruminations would involve focusing on the internally-driven salience network.

### Conclusions

Using EEG Theta/Alpha NeuroFeedback (T/A-NF) along with simultaneous fMRI, we identified four different periods that designated the neural dynamics of the transition into pre-sleep. We found that pre-sleep initiation depends on reduced activation in sub cortical regions involved in sensory gating (e.g. medial thalamus). In contrast, for sustainment of the pre-sleep state, opposite activation of anterior versus posterior salience network was necessary. This opposition possibly stands for shifting from extra- to intrapersonal neural processing, respectively. Revealing the underlying systems' dynamics of the transition from full awake towards falling asleep might serve brain-targeted diagnostic and therapeutic of sleep disorders.

Supplementary data to this article can be found online at <http://dx.doi.org/10.1016/j.neuroimage.2014.04.044>.

### Acknowledgments

Support for this research was provided by the U.S. Department of Defense award number W81XWH-11-2-0008 and from the Israeli Defense Forces Medical Corps and Israeli Ministry of Defense Funding Program for Research in Military Medicine. We thank A. Solski for assistance in manuscript preparation.

### References

Aftanas, L.I., Varlamov, A.A., Pavlov, S.V., Makhnev, V.P., Reva, N.V., 2001. Affective picture processing: event-related synchronization within individually defined human theta band is modulated by valence dimension. *Neurosci. Lett.* 303, 115–118.

Augner, C., 2011. Associations of subjective sleep quality with depression score, anxiety, physical symptoms and sleep onset latency in students. *Cent. Eur. J. Public Health* 19, 115–117.

Ben-Simon, E., Podlipsky, I., Arieli, A., Zhdanov, A., Hendler, T., 2008. Never resting brain: simultaneous representation of two alpha related processes in humans. *PLoS One* 3, e3984.

Bodizs, R., Sverteczki, M., Lazar, A.S., Halasz, P., 2005. Human parahippocampal activity: non-REM and REM elements in wake–sleep transition. *Brain Res. Bull.* 65, 169–176.

Buckner, R.L., Andrews-Hanna, J.R., Schacter, D.L., 2008. The brain's default network: anatomy, function, and relevance to disease. *Ann. N. Y. Acad. Sci.* 1124, 1–38.

Calcagnini, G., Biancalana, G., Giubilei, F., Strano, S., Cerutti, S., 1994. Spectral analysis of heart rate variability signal during sleep stages. *Engineering in Medicine and Biology Society, 1994. Engineering Advances: New Opportunities for Biomedical Engineers. Proceedings of the 16th Annual International Conference of the IEEE*, vol. 1252, pp. 1252–1253.

Coffman, K.A., Dum, R.P., Strick, P.L., 2011. Cerebellar vermis is a target of projections from the motor areas in the cerebral cortex. *Proc. Natl. Acad. Sci. U. S. A.* 108, 16068–16073.

Coizet, V., Comoli, E., Westby, G.W., Redgrave, P., 2003. Phasic activation of substantia nigra and the ventral tegmental area by chemical stimulation of the superior colliculus: an electrophysiological investigation in the rat. *Eur. J. Neurosci.* 17, 28–40.

De Gennaro, L., Ferrara, M., Bertini, M., 2001. The boundary between wakefulness and sleep: quantitative electroencephalographic changes during the sleep onset period. *Neuroscience* 107, 1–11.

Delorme, A., Makeig, S., 2004. EEGLAB: an open source toolbox for analysis of single-trial EEG dynamics including independent component analysis. *J. Neurosci. Methods* 134, 9–21.

Fiset, P., Paus, T., Daloz, T., Plourde, G., Meuret, P., Bonhomme, V., Hajj-Ali, N., Backman, S.B., Evans, A.C., 1999. Brain mechanisms of propofol-induced loss of consciousness in humans: a positron emission tomographic study. *J. Neurosci.* 19, 5506–5513.

Foley, D.J., Monjan, A.A., Brown, S.L., Simonsick, E.M., Wallace, R.B., Blazer, D.G., 1995. Sleep complaints among elderly persons: an epidemiologic study of three communities. *Sleep* 18, 425–432.

Ghelarducci, B., Sebastiani, L., 1996. Contribution of the cerebellar vermis to cardiovascular control. *J. Auton. Nerv. Syst.* 56, 149–156.

Gilbert, S.J., Dumontheil, I., Simons, J.S., Frith, C.D., Burgess, P.W., 2007. Comment on "Wandering minds: the default network and stimulus-independent thought". *Science* 317, 43 (author reply 43).

Hamilton, M., 1989. Frequency of symptoms in melancholia (depressive illness). *Br. J. Psychiatry* 154, 201–206.

Hammond, D.C., 2011. What is neurofeedback: an update. *J. Neurother.* 15, 305–336.

Han, S., Gu, X., Mao, L., Ge, J., Wang, G., Ma, Y., 2010. Neural substrates of self-referential processing in Chinese Buddhists. *Soc. Cogn. Affect. Neurosci.* 5, 332–339.

Hiroshige, Y., Miyata, Y., 1990. Slow eye movements and transitional periods of EEG sleep stages during daytime sleep. *Shinrigaku Kenkyu* 60, 378–385.

Hori, T., Hayashi, M., Morikawa, T., 1994. Topographical EEG changes and the hypnagogic experience. In: Ogilvie, R.D., Harsh, J.R. (Eds.), *Sleep Onset: Normal and Abnormal Processes*. American Psychological Association, Washington DC, pp. 237–254.

Horowitz, S.G., Fukunaga, M., de Zwart, J.A., van Gelderen, P., Fulton, S.C., Balkin, T.J., Duyn, J.H., 2008. Low frequency BOLD fluctuations during resting wakefulness and light sleep: a simultaneous EEG-fMRI study. *Hum. Brain Mapp.* 29, 671–682.

Johnson, M.L., Bodenhamer-Davis, E., Bailey, L.J., Gates, M.S., 2013. Spectral dynamics and therapeutic implications of the theta/alpha crossover in alpha-theta neurofeedback. *J. Neurother.* 17, 3–34.

Kinreich, S., Podlipsky, I., Intrator, N., Hendler, T., 2012. Categorized EEG neurofeedback performance unveils simultaneous fMRI deep brain activation. In: Langs, G., Rish, I., Grosse-Wentrup, M., Murphy, B. (Eds.), *Machine Learning and Interpretation in Neuroimaging*. Springer, Berlin Heidelberg, pp. 108–115.

Kjaer, T.W., Law, I., Wiltzschiotz, G., Paulson, O.B., Madsen, P.L., 2002. Regional cerebral blood flow during light sleep—a H(2)(15)O-PET study. *J. Sleep Res.* 11, 201–207.

Kleitman, N., 1963. *Sleep and Wakefulness*. University of Chicago Press.

Larson-Prior, L.J., Zempel, J.M., Nolan, T.S., Prior, F.W., Snyder, A.Z., Raichle, M.E., 2009. Cortical network functional connectivity in the descent to sleep. *Proc. Natl. Acad. Sci. U. S. A.* 106, 4489–4494.

Larson-Prior, L.J., Power, J.D., Vincent, J.L., Nolan, T.S., Coalson, R.S., Zempel, J., Snyder, A.Z., Schlaggar, B.L., Raichle, M.E., Petersen, S.E., 2011. Modulation of the brain's functional network architecture in the transition from wake to sleep. *Prog. Brain Res.* 193, 277–294.

Lyons, K.E., Zelazo, P.D., 2011. Monitoring, metacognition, and executive function: elucidating the role of self-reflection in the development of self-regulation. *Adv. Child Dev. Behav.* 40, 379–412.

Malik, M., 1996. Heart rate variability standards of measurement, physiological interpretation, and clinical use. *Eur. Heart J.* 17, 354–381.

Malik, M., 2007. Standard measurement of heart rate variability. *Dynamic Electrocardiography*. Blackwell Publishing pp. 13–21.

Marzano, C., Fratello, F., Moroni, F., Pellicciari, M.C., Curcio, G., Ferrara, M., Ferlazzo, F., De Gennaro, L., 2007. Slow eye movements and subjective estimates of sleepiness predict EEG power changes during sleep deprivation. *Sleep* 30, 610–616.

Menon, V., Uddin, L.Q., 2010. Saliency, switching, attention and control: a network model of insula function. *Brain Struct. Funct.* 214, 655–667.

Moroni, F., Nobili, L., Curcio, G., De Carli, F., Tempesta, D., Marzano, C., De Gennaro, L., Mai, R., Francione, S., Lo Russo, G., Ferrara, M., 2008. Procedural learning and sleep hippocampal low frequencies in humans. *Neuroimage* 42, 911–918.

Neylan, T.C., Marmar, C.R., Metzler, T.J., Weiss, D.S., Zatzick, D.F., Delucchi, K.L., Wu, R.M., Schoenfeld, F.B., 1998. Sleep disturbances in the Vietnam generation: findings from a nationally representative sample of male Vietnam veterans. *Am. J. Psychiatry* 155, 929–933.

Niazy, R.K., Beckmann, C.F., Iannetti, G.D., Brady, J.M., Smith, S.M., 2005. Removal of fMRI environment artifacts from EEG data using optimal basis sets. *Neuroimage* 28, 720–737.

Olbrich, S., Mulert, C., Karch, S., Trenner, M., Leicht, G., Pogarell, O., Hegerl, U., 2009. EEG-vigilance and BOLD effect during simultaneous EEG/fMRI measurement. *Neuroimage* 45, 319–332.

- Peniston, E., Kulkosky, P., 1991. Alphatheta brainwave neurofeedback therapy for Vietnam veterans with combat related posttraumatic stress disorder. *Int. J. Med. Psychother.* 4, 47–60.
- Peniston, E.G., Dale, A.M., Deming, W.A., Kulkosky, P., 1993. EEG alpha-theta brainwave synchronization in Vietnam theater veterans with combat-related post-traumatic stress disorder and alcohol abuse. *Adv. Med. Psychother.* 6, 37–50.
- Picchioni, D., Fukunaga, M., Carr, W.S., Braun, A.R., Balkin, T.J., Duyn, J.H., Horovitz, S.G., 2008. fMRI differences between early and late stage-1 sleep. *Neurosci. Lett.* 441, 81–85.
- Raz, G., Winetraub, Y., Jacob, Y., Kinreich, S., Maron-Katz, A., Shaham, G., Podlipsky, I., Gilam, G., Soreq, E., Hendler, T., 2012. Portraying emotions at their unfolding: a multilayered approach for probing dynamics of neural networks. *Neuroimage* 60, 1448–1461.
- Schiff, N.D., Shah, S.A., Hudson, A.E., Nauvel, T., Kalik, S.F., Purpura, K.P., 2013. Gating of attentional effort through the central thalamus. *J. Neurophysiol.* 109, 1152–1163.
- Schreckenberger, M., Lange-Asschenfeld, C., Lochmann, M., Mann, K., Siessmeier, T., Buchholz, H.-G., Bartenstein, P., Gründer, G., 2004. The thalamus as the generator and modulator of EEG alpha rhythm: a combined PET/EEG study with lorazepam challenge in humans. *Neuroimage* 22, 637–644.
- Shirer, W.R., Ryali, S., Rykhlevskaia, E., Menon, V., Greicius, M.D., 2012. Decoding subject-driven cognitive states with whole-brain connectivity patterns. *Cereb. Cortex* 22, 158–165.
- Shulman, G.L., Fiez, J.A., Corbetta, M., Buckner, R.L., Miezin, F.M., Raichle, M.E., Petersen, S.E., 1997. Common blood flow changes across visual tasks: II. Decreases in cerebral cortex. *J. Cogn. Neurosci.* 9, 648–663.
- Sokhadze, T.M., Cannon, R.L., Trudeau, D.L., 2008. EEG biofeedback as a treatment for substance use disorders: review, rating of efficacy, and recommendations for further research. *Appl. Psychol. Biofeedback* 33, 1–28.
- Sridharan, D., Levitin, D.J., Menon, V., 2008. A critical role for the right fronto-insular cortex in switching between central-executive and default-mode networks. *Proc. Natl. Acad. Sci. U. S. A.* 105, 12569–12574.
- Stockwell, R.G., Mansinha, L., Lowe, R.P., 1996. Localization of the complex spectrum: the S transform. *IEEE Trans. Signal Process.* 44, 998–1001.
- Trinder, J., Kleiman, J., Carrington, M., Smith, S., Breen, S., Tan, N., Kim, Y., 2001. Autonomic activity during human sleep as a function of time and sleep stage. *J. Sleep Res.* 10, 253–264.
- Uusberg, A., Thiruchselvam, R., Gross, J.J., 2014. Using distraction to regulate emotion: insights from EEG theta dynamics. *Int. J. Psychophysiol.* 91, 254–260.
- Wang, X., Jin, J., Jabri, M., 2002. Neural network models for the gaze shift system in the superior colliculus and cerebellum. *Neural Netw.* 15, 811–832.
- Ward, L.M., 2011. The thalamic dynamic core theory of conscious experience. *Conscious. Cogn.* 20, 464–486.
- Worsnop, C., Kay, A., Pierce, R., Kim, Y., Trinder, J., 1998. Activity of respiratory pump and upper airway muscles during sleep onset. *J. Appl. Physiol.* 85, 908–920.
- Xue, G., Lu, Z., Levin, I.P., Bechara, A., 2010. The impact of prior risk experiences on subsequent risky decision-making: the role of the insula. *Neuroimage* 50, 709–716.